Preprint
UCRL-JC-137418

Effects of Confinement on Combustion of TNT Explosion Products in Air

A.L. Kuhl, A.K. Oppenheim, R.E. Ferguson, H. Reichenbach and P. Neuwald

This article was submitted to
28th International Symposium on Combustion, Edinburgh, Scotland, July 30 – August 4, 2000

U.S. Department of Energy
Lawrence Livermore National Laboratory

February 5, 2000

Twenty Eighth International Symposium on Combustion

*EFFECTS OF CONFINEMENT ON COMBUSTION OF TNT EXPLOSION PRODUCTS IN AIR

A.L. Kuhl†, A.K. Oppenheim*, R. E. Ferguson#, H. Reichenbach‡ & P. Neuwald‡

†Lawrence Livermore National Laboratory, Livermore, CA
*University of California, Berkeley, CA
#Krispin Technologies Inc, Rockville, MD
‡Ernst Mach Institut, Freiburg

Corresponding author

A.L Kuhl, Ph.D.

Lawrence Livermore National Laboratory
P. O. Box 808, Livermore, CA 94550 USA
Phone: (925) 422-4777
FAX: (925) 423-9969
Email: kuhl2@llnl.gov

Colloquium

Detonations, Propellants and Supersonic Combustion

Word count

Text (computer count):		1880	
References (computer count)		411	
12 Figures & 2 Tables	14x200=	2800	
Equations	13x21=	273	
Total:		5364	(5500 allowable)

*This work was performed under the auspices of the auspices of the U.S. Department of Energy by the University of California Lawrence Livermore National Laboratory under contract No. W-7405-Eng-48.

Abstract

Turbulent combustion fields established by detonative explosions of TNT in confinements of different sizes are studied by high-resolution numerical simulation, using AMR (Adaptive Mesh Refinement) method. The chambers are filled with nitrogen or air at NPT conditions. In the second case, the detonation products, rich in C and CO, act, upon turbulent mixing with air, as fuel in an exothermic process of combustion, manifested by a distinct pressure rise. It is the evolution in space and time of this dynamic process that formed the principal focus of this study. Our results demonstrate a dominating influence of the size of the enclosure on the burning rate—an effect that cannot be expressed in terms of the classical burning speed. Under such circumstances, combustion is of considerable significance, since it is associated with a calorific value ("heat release") of an order of 3500 Cal/gm, as compared to 1100 Cal/gm of TNT detonation. The numerical simulations provide considerable insight into the evolution of combustion fields dominated by shock-turbulence interactions. Fuel consumption histories, extracted from the simulations, reveal the dynamic features of the system, represented by the rate of combustion (akin to velocity) and its change (akin to acceleration). Time profiles of the mass fraction of consumed fuel are expressed, with a remarkable accuracy, by bi-parametric life functions, whereby the trajectories of these parameters, obtained by differentiation, can be evaluated with precision commensurate with their commanding role in the identification of the dynamic nature of the system.

[245 words]

Abstract

A numerical study of turbulent combustion following detonative explosions of TNT in geometrically similar cylinders filled with air reveals that the combustion rate depends significantly on the size of confinement. The fluid-dynamic solution provides an insight into the evolution of combustion fields dominated by strong interactions between turbulence and shock waves. Time profiles of fuel consumption, extracted from this solution, demonstrate the dynamic (thermokinetic) features of the system, expressed by the rate of combustion (akin to velocity) and its change (akin to acceleration). Their evolution is described by means of bi-parametric life functions.

Question

The focus of this study is the dynamic stage of combustion, manifested by pressure rise, associated with an escalating rate of burn, following an explosion. This phenomenon is of appreciable significance because the calorific value for a conventional explosive, like TNT, is of an order of 3500 Cal/gm, whereas that of its detonation is only around 1000 Cal/gm (Ornellas [1]). For this reason such a post-explosion combustion of this kind became well known as "after-burn" (Dewey [2]), and attracted a good deal of attention—attested by a number of recent bomb calorimeter tests itemized in Table 1, with their background provided in [5].

The question is, under such circumstances: *"What is the effect of confinement on the evolution of the exothermic process of such a post-explosion combustion?"* Specifically this is expressed in terms of the thermokinetic parameters: the rate of fuel consumption (i.e. rate of burn akin to velocity) and its change (akin to acceleration). Such global parameters cannot be measured, since they pertain to integral quantities of a highly turbulent field affected by shocks. The most direct way to answer this question is through numerical simulations.

Formulation

The confined TNT explosions were modeled as turbulent combustion in an unmixed system [7] consisting of hot fuel (expanded detonation products gases) which is oxidized by air to form combustion products. We consider the asymptotic limit of large Reynolds, Peclet and Damköhler numbers, where the influence of transport processes become negligible [8]. This results in a three-component gasdynamic model [9], which contains stoichiometric source/sink terms for component mass fractions and energy. This same methodology has been used

successfully to simulate mixing in spherical HE fireballs [10], combustion of a hot acetylene jet in air [11], and combustion of TNT explosion products in a 17-m^3 tank [6,12]. The numerical solution was obtained by a high-order Godunov scheme [13]; Adaptive Mesh Refinement [14] was used to trace the turbulent mixing in as much detail as possible.

A confined explosion problem was formulated by assuming that a 1-g sphere of TNT detonates in a circular cylinder with half-height equal to radius ($H/2=R$). A two-dimensional (r-z) grid was used, where the cylinder walls were modeled by inviscid (slip flow) boundary conditions. Only one quadrant of the problem was calculated, corresponding to the domain: $0 \le r \le R$ and $0 \le z \le H/2$. Four geometrically similar chambers were considered, which spanned the energy-per-unit-volume covered by experiments delineated in Table 1. **Case 1** (R = 6 cm) is typical of the highly-confined explosions found in bomb calorimeters. **Case 2** (R = 10 cm) is representative of explosions in the "1-kg Tank" at Lawrence Livermore National Laboratory (LLNL). **Case 3** (R = 20 cm) is similar to model experiments performed at the Ernst Mach Institut (EMI). **Case 4** (R = 40 cm) corresponds to a virtually unconfined explosion. Each case involved two simulations: (i) detonation in a nitrogen atmosphere, referred to as explosion (subscript E); and (ii) detonation in air, referred to as combustion (subscript C). Time histories of mean (volume-averaged) pressures and mass fractions of fuel were deduced from the numerical solution. The pressure due to after-burning (A) was then evaluated as the difference: $p_A(t) = p_C(t) - p_E(t)$.

Simulations

Figure 1 presents a comparison of the combustion fields of Cases 1-4 at the same time of 0.6 ms. There, fuel (TNT detonation products) is represented as yellow, air is blue, and combustion products are red. White dots denote the currently-reacting exothermic cells. Black lines indicate shocks fronts, while vorticity is visualized by turquoise (positive) and chartreuse (negative) contours. White dotted-line boxes delineate AMR grid patches. In Case 1, the combustion is virtually complete, based on the visible amount of red products. In Case 2, about half the fuel has been consumed; combustion is distributed throughout the chamber (a "distributed combustion mode") due to shock-enhanced mixing. In Case 3, only 15% of the fuel has been consumed; the primary and secondary shocks have reflected from the chamber walls, but have not yet reached the mixing layer; combustion is therefore limited to exothermic sheets near the surface of mixing layer. In Case 4, the primary, secondary and tertiary spherical shock

waves induced by the expansion of the TNT products gases are clearly visible; they have not yet reflected from the chamber walls, so fuel consumed is similar to Case 3.

Pressure histories at points in space are very noisy, due to the shock reverberations; instead we report mean (volume-averaged) gauge pressure histories $p_g(t)$ which are presented in Figs. 2-5. Each contains three curves: $p_E(t)$ corresponding to explosion, $p_C(t)$ to combustion, and $p_A(t)$ to after-burning, respectively. Mean pressures start out equal, but diverge at late times due to combustion. The chamber pressure in Case 1 reached a maximum value of $p_m = 19.1$ bars in air versus $p_e = 9.44$ bars in nitrogen; in Case 2, $p_m = 7.28$ bars versus $p_e = 2.31$ bars; in Case 3, $p_m = 1.06$ bars versus $p_e = 0.307$ bars; and in Case 4, $p_m = 0.134$ bars versus $p_e = 0.0373$ bars. The combustion cases have been non-dimensionalized by p_e and plotted in Fig. 6. The results demonstrate that combustion increases the maximum pressures in the chamber by a factor of about 3.5, regardless of the chamber volume.

Profiles of mass fractions of fuel, $\mu(t) \equiv 1 - \int_V \rho_F dV' / M_F$, consumed in the course of the dynamic stage of combustion (vid. start of next section), are displayed for the four cases in Fig. 7. In Case 1, the size of the container was apparently too small to accommodate enough air, so that combustion was terminated when only about half of the fuel produced by explosion was burned. Although all cases start begin with the same high burning rate, this figure conclusively illustrates that the fuel consumption rate depends on chamber size.

Thermokinetics

Life function

The results described above pertain to the dynamic stage of the exothermic process in a closed combustion system, manifested by pressure rise and a concomitant consumption of fuel. The latter is expressed in terms of the its mass fraction with respect to the fuel supplied to the system, $\mu(t)$. The thermokinetic parameters of this system are most appropriately expressed in terms of a life function [15,16]:

$$x_k = \frac{e^{\zeta} - 1}{e^{\zeta_f} - 1} \tag{1}$$

where k = P, F, for, respectively, over-pressure and fuel consumed in the course of the dynamic stage of combustion, both normalised by their maximum values, while, with respect to the life time $T \equiv t_f - t_i$, $\tau \equiv (t - t_i)/T$ as the independent variable,

$$\zeta \equiv \frac{\alpha}{\chi + 1}[1 - (1 - \tau)^{\chi+1}] \tag{2}$$

The case at hand this means that $x_p \equiv p_C/p_m$, while $x_F = \mu$. This expression is the reverse of the so-called 'Wiebe' [17,18,19] — alias of Vibe [20,21] — function. It should be noted that μ_f expresses the efficiency with which fuel is utilised in the course of the dynamic stage of combustion.

In contrast to the 'Wiebe' function, according to (1), $\dot{x} > 0$, while $\dot{x}_f = 0$, where i and f denote the initial and final point receptively. The rate of fuel consumption (akin to velocity in a dynamic system) is then, with Newtonian dots referring to derivatives with respect to τ, given by

$$\dot{x} = \alpha(\xi + x)(1 - \tau)^{\chi} \qquad (\chi > 0) \tag{3}$$

while its change (akin to acceleration) is

$$\ddot{x} = (\xi + x)(\dot{\zeta}^2 + \ddot{\zeta}) \tag{4}$$

wherefore

$$\dot{\zeta} = \alpha(1 - \tau)^{\chi} \tag{5}$$

and

$$\ddot{\zeta} = -\alpha\chi(1 - \tau)^{\chi-1} = \frac{-\chi}{1 - \tau}\dot{\zeta} \tag{6}$$

The life function plots as an S-curve. At the point of inflection, i.e. @ $\ddot{x} = 0$,

$$\alpha(1 - \tau^*)^{\chi+1} - \chi = 0 \tag{7}$$

so that

$$\tau^* = 1 - (\chi/\alpha)^{1/(\chi+1)} \tag{8}$$

and

$$\zeta^* = \frac{\alpha - \chi}{\chi + 1} \tag{9}$$

Provided thus is a criterion for distinguishing between two types of events: **mild initiation**, corresponding

to $\tau^* > 0$, which takes place for $0 < \chi < \alpha$, and **strong initiation** when $\tau^* < 0$ that occurs for $\chi > \alpha$.

Extra Strong Initiation

Following an explosion, the initiation of combustion is extra strong. The dynamic stage of combustion (its active life) is then much shorter than its total lifetime, the decay to the terminal state (death) being extremely slow. Thus, the period of interest in this case, $\Delta t << T$, or $\tau << 1$. As implied then by empirical evidence, the independent variable acquires then a power-law dependence on time, i.e. $\tau \equiv t/T^{\delta}$, where $\delta \leq 1$. By grouping the lifetime with the rate parameter, so that $\Lambda \equiv \alpha/T^{\delta}$, it is taken out of scope. As a consequence of the domineering influence of the first term in the series expansion of $\zeta(\tau)$, it is reduced then to linear function, whereby the power parameter, χ, is eliminated, so that

$$\zeta = \alpha\tau = \Lambda t^{\delta} \tag{10}$$

while, noting that here $t_f = \infty$,

$$x = 1 - e^{-\zeta} = 1 - \exp(-\Lambda t^{\delta}) \tag{11}$$

The problem is thus expressed in terms of two parameters, Λ and δ, replacing α and χ used before, while the role of independent variable is taken over by t. Then, with Newtonian dot expressing this time differentiation with respect to it, it follows from (11) that

$$\dot{x} = \Lambda\delta(1-x)t^{\delta-1} \tag{12}$$

whence, if $\delta < 1$, then $\dot{x}_i = \infty$; if $\delta = 1$, $\dot{x}_i = \Lambda$; and for $\delta \leq 1$, $\dot{x}_f = 0$, while

$$\ddot{x} = -[\Lambda\delta t^{\delta-1} - (\delta-1)t^{-1}]\,\dot{x} = -[\Lambda\delta t^{\delta} - (\delta-1)]\,\dot{x}t^{-1} \tag{13}$$

so that $\ddot{x}_i = -\infty$, and $\dot{x}_f = 0$.

Thus, all the thermokinetic (dynamic) properties of the combustion field are expressed in terms of two parameters, α and χ in the case of normal life function, Λ and δ in that of its form for extra strong initiation.

Implementation

Life functions, matching the calculated fuel consumption profiles displayed in Fig. 7, are presented by Figs. 8 and 9. Their parameters are listed in Table 2. In Case 1 the efficiency of the utilization of fuel was $\mu_f = 0.5$, as a consequence of an insufficient amount of air available within the relatively small chamber volume. As depicted in Fig. 8, this case, as well as case 2, exhibit profiles characteristic of extra-strong initiation (11) throughout their life. As displayed in Fig.9, the evolutions of cases 3 and 4 consist of two stages. They also start on an exponential curve

(marked by 3.1 and 4.1) corresponding to extra-strong initiation, but eventually they become influenced by shock reflections from the walls, and thereby acquire the character of a normal life function (see curves 3.2 and 4.2). This cross-over time depends on the chamber size.

Conclusions

The burning rate for combustion of TNT explosion products in air depends on the chamber size. This effect is caused by shock reflections from the walls, which modify the mixing and entrainment—thereby changing the combustion rate. Mean pressure histories induced by combustion of TNT products are shown to scale as $p_C(t)/p_e$, and reach an asymptotic value 3.5 times larger than the explosion case—regardless of the chamber volume—as long as there is enough air to oxidize all the fuel.

The evidently excellent match of the life functions with the calculated mass fractions of consumed fuel demonstrate their value as useful diagnostic tool to extract global information on the dynamic properties of the reacting system from the results of multi-dimensional numerical simulations. Revealed thus are the salient features of the mechanism of the process, expressed in specific terms of its parameters, which are not provided by the detailed structure of the field obtained by the fluid dynamic simulations.

Acknowledgements

This research was performed under the auspices of the U.S. Department of Energy by Lawrence Livermore National Laboratory under contract #W-7405-Eng-48. This work was sponsored by the U.S. Defense Threat Reduction Agency under IACRO Number 98-3016.

REFERENCES

1. Ornellas, D. L., "Calorimetric Determination of the Heat and Products of Detonation for Explosives: October 1961 to April 1982", Lawrence Livermore National Laboratory, **UCRL-52821**, Livermore, CA, 1982.
2. Dewey, J. M., *Proc. Roy. Soc.—Series A* 279:366-385 (1964).
3. Cudzilo, S., Paszula, J., Trebinski, R., Trzcinski, W., and Wolanski, P., *Int. Symp. on Hazards, Prevention & Mitigation of Industrial Explosions*, Vol. 2, Safety Consulting Engineers, Schaumburg, IL, 1998, pp. 50-67.
4. Wolanski, P., Gut, Z., Trzcinski, W. A., Szymanczyik, L., Paszula, J., *17th Int. Colloquium on Dynamics of Explosions and Reactive Systems*, Heidelberg, 1999, ISBN 3-932217-01-2, 1999 (submitted to *Shock Waves*).
5. Neuwald, P., Reichenbach, H., and Kuhl, A. L., *17th Int. Colloquium on Dynamics of Explosions and Reactive Systems*, Heidelberg, 1999, ISBN 3-932217-01-2.
6. Kuhl, A.L, Forbes, J, Chandler, J., Oppenheim, A.K., and Ferguson, R.E., *Int. Symp. on Hazards, Prevention & Mitigation of Industrial Explosions*, Vol. 2, Safety Consulting Engineers, Schaumburg, IL, 1998, pp. 1-49.
7. Zel'dovich, Ya. B., *Zh. Tekh. Fiz.*, 19(10):1199-1210 (1949).
8. Kuhl, A. L., and Oppenheim, A.K., *Advanced Computation and Analysis of Combustion*, ENAS Publishers, Moscow, 1997, pp. 388-396.
9. Kuhl, A. L., Ferguson, R. E., and Oppenheim, A. K., *Advances in Combustion Science—in Honor of Ya. B. Zel'dovich: Prog. in Astronautics and Aeronautics Series*, 173, AIAA, Washington DC, 1997, pp. 251-261.
10. Kuhl, A. L., *Dynamics of Exothermicity*, Gordon and Breach, Longhorn, PA, 1996, pp. 291-320.
11. Kuhl, A. L., Ferguson, R. E., Reichenbach, H., Neuwald, P., and Oppenheim, A.K., *JSME Int. Journal-Series B*, 41(2): 416-423 (1998).
12. Kuhl, A.L., Ferguson, R.E., and Oppenheim, A.K., "Gasdynamics of Combustion of TNT Products in Air", *Archivum Combustionis* (in press).
13. Colella, P. and Glaz, H. M., *J. Comp. Phys.* 59(2):264-289 (1985).
14. Bell, J. B., Berger, M., Saltzman, J., Welcome, M. *SIAM J. Sci. & Stat. Comp.* 15(1):127-138 (1994).
15. Oppenheim, A.K. & Kuhl, A.L., *Modeling of SI & Diesel Engines SAE SP-1330*, # 980780, 1998, pp.75-84.
16. Oppenheim, A.K. and Kuhl, A.L., "Energy Loss from Closed-Combustion Systems" (submitted to *28th Int. Symposium on Combustion)*.
17. Jante, A., *Kraftfahrzeugtchnik*, 9:340 – 346, 1960.
18. Gatowski, J.A., Balles, E.N., Chun, K.M., Nelson, F.E., Ekchian, J.A. & Heywood, J.B., *SAE #841359 (*1984).
19. Heywood, J.B., Higgins, J.M., Watts, P.A. and Tabaczynski, R.J., *SAE Paper 790291*, 26 pp.(1979).
20. Vibe, I.I., *Conference on Piston Engines*, USSR Academy of Sciences, Moscow, 1956, pp. 185-191.
21. Vibe, I.I. *Brennverlauf und Kreisprozess von Verbrennungsmotoren* VEB Verlag Technik, Berlin, 1970, 286 pp.

Table 1. Chambers for after-burning experiments

MUT Calorimeter [3]

- M = 25g, 50g & 100g TNT sphere in V =3-l air
  $\Leftrightarrow$ 31< V(cc/g) <124 & 2< R(cm/g$^{1/3}$) <3

LLNL Calorimeter [1]

- M = 25g TNT sphere in V =5.3-l of 2.5-b O_2
  $\Leftrightarrow$ V = 210-cc/g & R = 3 cm/g$^{1/3}$

EMI Calorimeter [5]

- M = 0.2g-1g PETN sphere in V = 603cc air
  $\Leftrightarrow$ 600< V(cc/g) <3000 & 5< R(cm/g$^{1/3}$) <8

LLNL 1-kg Tank [6]

- M =875g TNT cylinder in V = 16.6m^3 air & N_2
  $\Leftrightarrow$ V = 19,000 cc/g & R = 14.5 cm/g$^{1/3}$

EMI Model

- M = 0.2g-1g PETN sphere in V = 13,500cc air

$\Leftrightarrow$ 13,500< V(cc/g) <67,500 & 13< R(cm/g$^{1/3}$) <22

WUT Explosion Visualization Chamber [4]

- M = 0.5g-1.27g TNT in V = 107,000cc air

$\Leftrightarrow$ 84,000< V(cc/g) <107,000 & 24< R(cm/g$^{1/3}$) <32

Table 2. Parameters of life functions

Case	Λ	δ	μ_e	α	χ	T
1	0.82	0.56	0.51			
2	1.3	1	1			
part:	1			2		
3	0.4	0.8	0.25	23	5.8	6.6
4	0.3	0.5	0.31	6	3.8	14

Figures

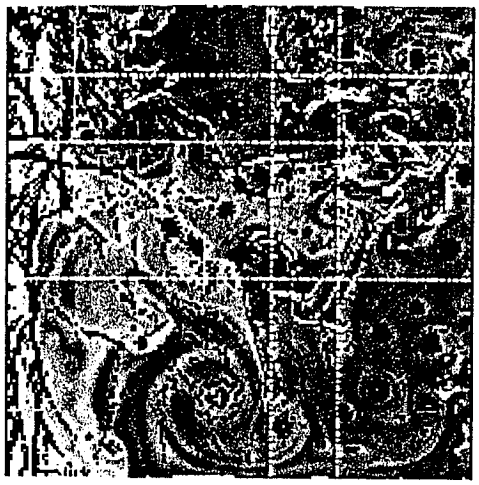

(a) Case 1: $0 < r < 6cm$; $0 < z < 6cm$

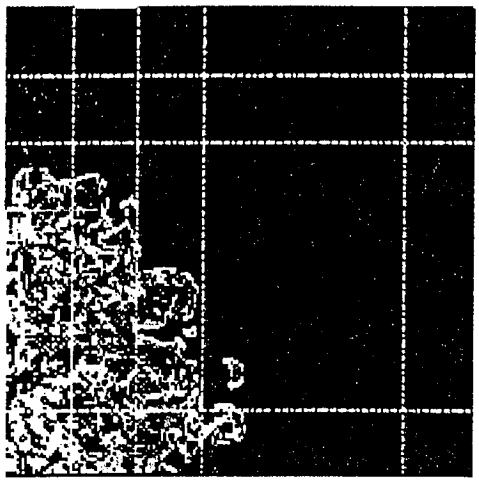

(c) Case 3: $0 < r < 20cm$; $0 < z < 20cm$

(b) Case 2: $0 < r < 10cm$; $0 < z < 10cm$

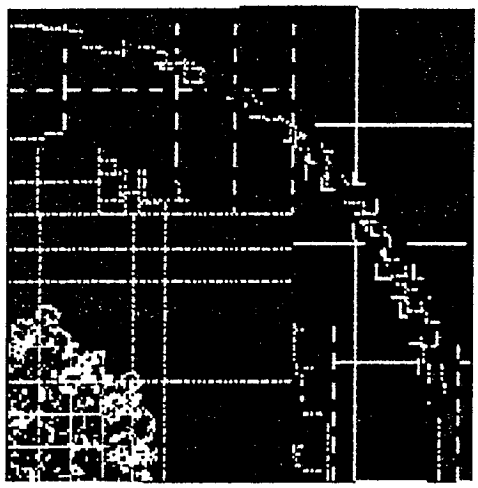

(d) Case 4: $0 < r < 40cm$; $0 < z < 40cm$

Figure 1. Cross-sectional view of the flow field at t = 0.6 ms (see text for extended comments).

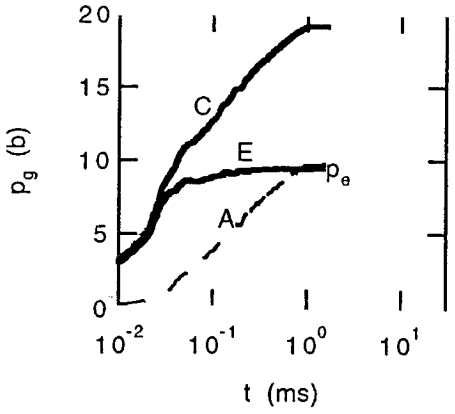

Fig. 2 Mean pressure histories (Case 1).

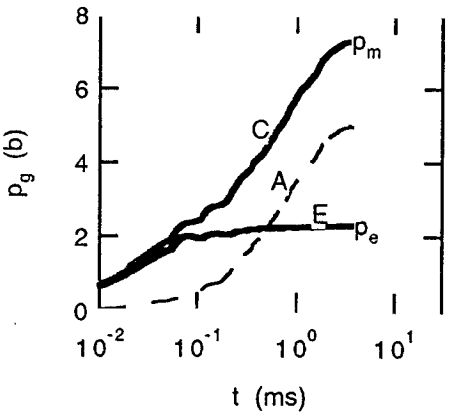

Fig. 3 Mean pressure histories (Case 2).

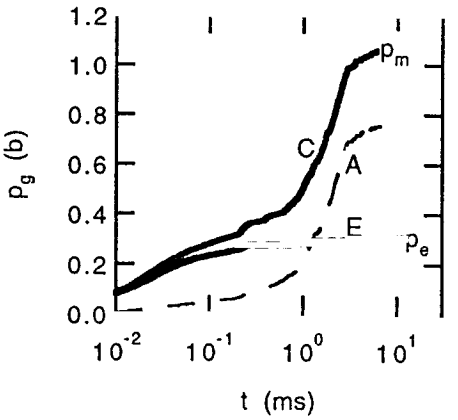

Fig. 4 Mean pressure histories (Case 3).

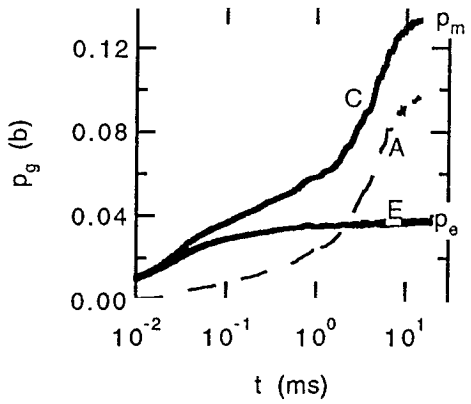

Fig. 5 Mean pressure histories (Case 4).

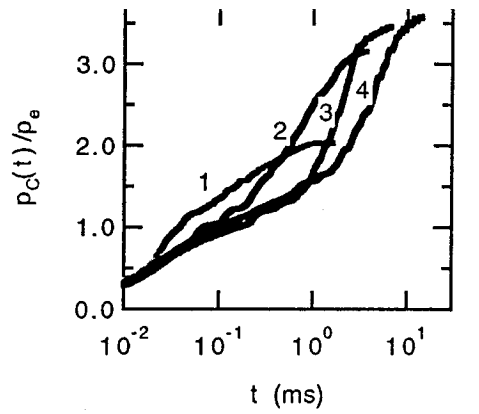

Fig. 6 Scaled pressure histories induced by combustion (Cases 1,2,3 & 4).

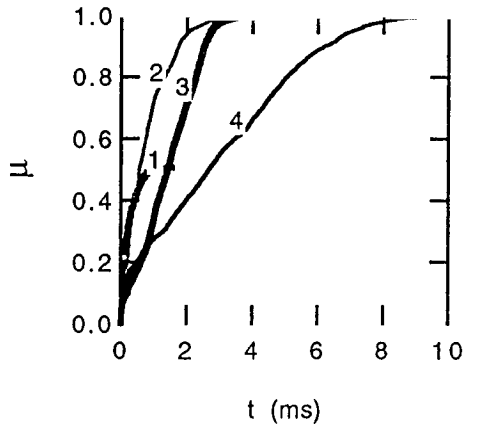

Fig. 7 Mass fraction of fuel consumed by combustion (Cases 1,2,3 & 4).

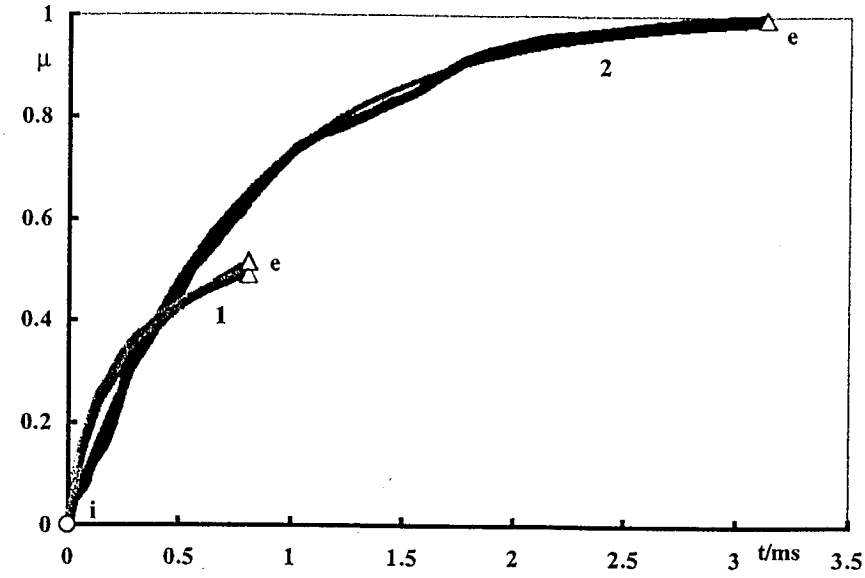

Fig. 8 Mass fraction of fuel consumed for strong confinement (Cases 1 and 2).

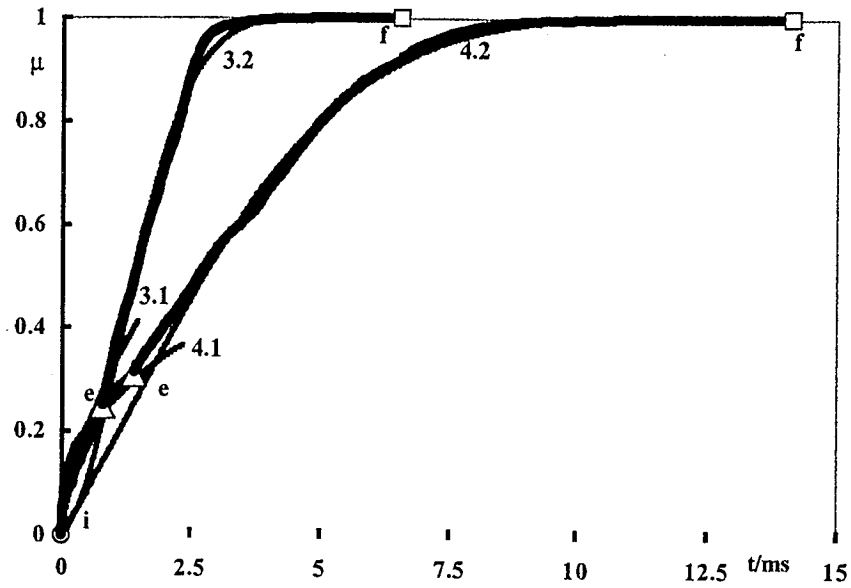

Fig. 9 Mass fraction of fuel consumed for weaker confinement (Cases 3 and 4).